

Local Einstein relation for fractals

L. Padilla, J. L. Iguain

Instituto de Investigaciones Físicas de Mar del Plata (IFIMAR) and
Departamento de Física FCEyN, Universidad Nacional de Mar del Plata,
Deán Funes 3350, 7600 Mar del Plata, Argentina

E-mail: iguain@mdp.edu.ar

Abstract. We study single random walks and the electrical resistance for fractals obtained as the limit of a sequence of periodic structures. In the long-scale regime, power laws describe both the mean-square displacement of a random walk as a function of time and the electrical resistance as a function of length. We show that the corresponding power-law exponents satisfy the Einstein relation. For shorter scales, where these exponents depend on length, we find how the Einstein relation can be generalized to hold locally. All these findings were analytically derived and confirmed by numerical simulations.

Keywords: Fractals, Power-law behaviours, Einstein relation.

1. Introduction

Fractals are characterized by quantities that exhibit power-law behaviour in space or time. More precisely, as scale invariance occurs for integer powers of a characteristic length, pure power laws are modulated by logarithmic periodic functions, that describe the departures from the main trend at intermediate scales. These modulations have been the object of recent interest and considerable effort has been devoted toward understanding the relation between log-periodicity and discrete-scale invariance [1–13].

For a given fractal and some related observables, which show (modulated) power-law behaviours, a problem of interest is to determine whether or not the exponents associated with these quantities are independent. Sometimes we can expect a relation as a consequence of underlying physical laws. This is, for example, the case of the mass m , the electric resistance R and the mean-square-displacement (MSD) Δr^2 for a single random walker. On a fractal, the first two grow with length l as $m(l) \sim l^{d_f}$ and $R(l) \sim l^\zeta$, while the last one grows with time t as $\Delta r^2(t) \sim t^{2/d_w}$. The exponents d_f , ζ and d_w are known as the *fractal*, *resistance* and *walk* exponents, respectively, and these power-law behaviours hold for scales large enough to ensure self-similarity. In an d -dimensional euclidean space, the diffusion coefficient D and conductivity σ are related by the Einstein equation [14]

$$\sigma = \frac{e^2 \rho}{k_B T} D. \quad (1)$$

Here, $D = \lim_{t \rightarrow \infty} \Delta r^2(t)/2t$, ρ and e are the density and charge of mobile particles, T is the temperature and k_B is the Boltzmann constant. Equation (1) is one of the forms of the fluctuation-dissipation theorem, and can be used together with simple scaling heuristic arguments, to argue that the fractal, walk, and resistance exponents satisfy the *Einstein relation* [14]

$$d_f = d_w - \zeta, \quad (2)$$

This property has been shown to hold asymptotically for some finitely ramified fractals [15, 16]; which has been used to analyze the periodicity of the oscillations in dynamic observables, in the first attempts to understand log-periodic modulation [17]. Einstein relation was also investigated for random walks on weighted graphs [18], and, more recently, for karst networks structures [19].

A deterministic fractal can be obtained as the limit of a sequence of periodic structures. In this procedure, the period increases at every step as L^n ($n = 0, 1, 2, \dots$), where L is a basic characteristic length scale. Self-similarity is manifested in power-law behaviours, which occur for long enough scales. However, this does not always hold for shorter lengths. Thus, the local slopes of the observables as a function of time or length, in log-log scales, are variable quantities, which approach constant values only asymptotically.

In this work we argue that the local fractal, walk, and resistance exponents are related through an equation that generalizes (2). This generalization is obtained

analytically, following the steady-state method for the calculation of the effective diffusion coefficients for periodic substrates [20]. To further strengthen our findings we perform numerical simulations for two models of fractals; which confirm the theoretical predictions.

The paper is organized as follows. In Sec. 2 we relate the diffusion coefficient and the unit cell resistance for a periodic structure. In Sec. 3 we derive the Einstein relation for self-similar systems. In Sec. 4 we generalize this relation for scale-dependent exponents. In Sec. 5 we confirm the generalized relation by numerical simulations performed on models of asymptotic self-similar substrates. Finally, we give our conclusions in Sec. 6.

2. Periodic systems

In this section we address the problem of the diffusion coefficient for a periodic substrate. We follow the steady-state method developed in reference [20]. We start by introducing the periodic substrate with unit cell of linear dimension l , schematized in figure 1, where the points represent sites, and the arrows represent hopping rates. On this structure, a mobile particle can jump between connected sites according to the hopping rates k 's (for the sake of clarity only a few sites and arrows were highlighted). We focus on a steady-state of non-interacting particles flowing with a constant current density j .

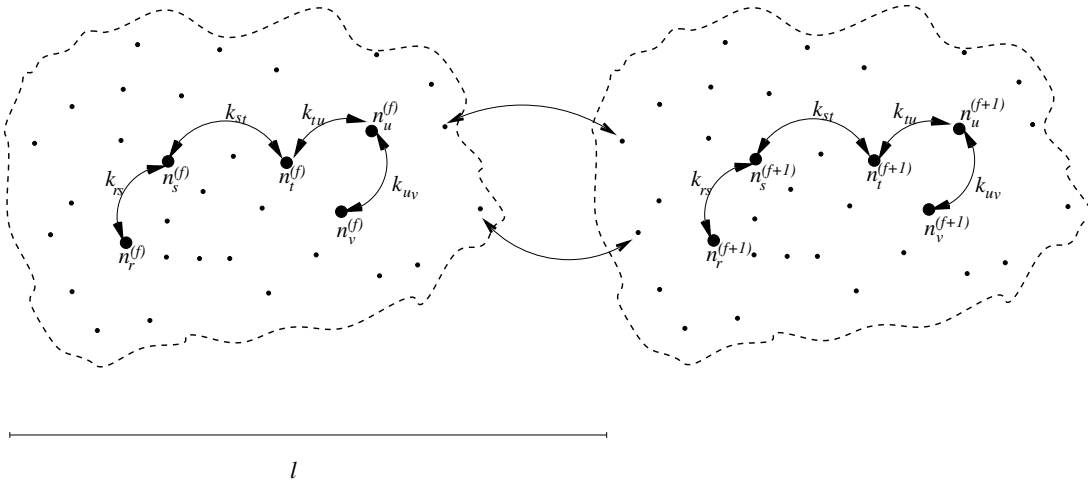


Figure 1. Two nearest-neighbor cells f and $f + 1$, for a periodic substrate with linear size period l . The points represent sites, which can be occupied by mobile particles. The arrows represent hopping rates between pairs of sites. For clarity, only a few sites and hopping rates were highlighted. $n_r^{(f)}$ corresponds to the number of particles in the internal site r of cell f

As shown in [20], this steady-state consists of a set of microscopic currents distributed with the same periodicity as the substrate. In figure 1 two nearest-neighbor (NN) unit cells are depicted schematically where, for example, $n_s^{(f)}$ represents the number of particles in site r (internal index) of cell f . Because of the mentioned

periodicity, we get that for given pair of connected sites with internal indices s and t ,

$$i_{rs}^{(f)} = i_{rs}^{(f+1)}, \quad (3)$$

where $i_{rs}^{(f)}$ is the current from site s to site r in cell f . In addition, as hopping rates do not depend on the cell either but only on the internal indices, the last equation can be rewritten as

$$k_{sr}(n_s^{(f)} - n_r^{(f)}) = k_{sr}(n_s^{(f+1)} - n_r^{(f+1)}), \quad (4)$$

or

$$n_s^{(f+1)} - n_s^{(f)} = n_r^{(f+1)} - n_r^{(f)}. \quad (5)$$

Therefore, in the steady-state, the difference in the occupation number for a given site and the equivalent site in a NN cell is the same for all sites.

The relation of the steady-state problem with the diffusion coefficient D is provided by Fick's law

$$j = -D \frac{\Delta n}{l^2}, \quad (6)$$

which is valid for distances larger than l . Here Δn corresponds to the particle number difference for NN cells. Note that D also determines the mean-square displacement $\Delta^2 x$ of a single random walker on the same structure, which behaves as

$$\Delta^2 x(t) = 2Dt; \quad (7)$$

for time long enough for $\Delta x \gg l$.

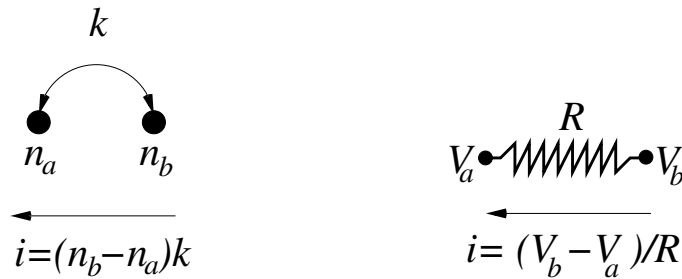


Figure 2. Schematics of the equivalence between Fick's law (left) and Ohm's law (right). In the mapping particles have unitary charge, while the other quantities are related as $V = n$, and $R = 1/k$.

Transforming the steady-state problem into an equivalent electrical problem is straightforward. Indeed, for particles of unitary electric charge, a mapping between Fick's law and Ohm's law results by identifying particle number with electrostatic potential ($V_a = n_a$) and hopping rate with conductance ($k = 1/R$). In figure 2 we represent this mapping for every pair of connected sites. Following this analogy, we see

that in the electric problem, the potential difference for a pair of equivalent sites in NN cells takes the constant value

$$\Delta V = n_r^{(i+1)} - n_r^{(i)}, \quad (8)$$

and that the difference between particle populations

$$\Delta n = \sum_{r=1}^M (n_r^{(i+1)} - n_r^{(i)}) = M \Delta V, \quad (9)$$

is proportional to the potential difference ΔV , where the constant of proportionality M corresponds to the number of sites per unit cell.

Thus, according to equation (6), we can conclude that, given a periodic substrate with unit cell of linear dimension l and M sites, the diffusion coefficient and the potential difference between two equivalent sites in NN cells, are connected through the relation

$$D = -j \frac{l^2}{M \Delta V}, \quad (10)$$

where j is the steady-state current density.

3. Self-similar substrates

Deterministic fractals are usually built by a recursive procedure, that results in a sequence of structures called *generations*. A generation consists of a periodic array of sites connected by bonds. The process begins with a basic periodic structure (zeroth generation). At every step the unit cell is scaled by a factor L and the building rules ensure that self-similarity is obtained after a large number of iterations.

Following equation (10), the diffusion coefficient D_p for the generation p and the potential difference ΔV_p between two equivalent points in NN unit cells are related as

$$D_p = -j \frac{L^{2p}}{M_p \Delta V_p}, \quad (11)$$

where M_p is the number of sites in the unit cell, and L^p is its linear dimension. Then, for two consecutive generations p and $p + 1$, through which the same steady-state current flows, we obtain

$$\frac{D_p}{D_{p+1}} = L^{-2} \frac{M_{p+1}}{M_p} \frac{\Delta V_{p+1}}{\Delta V_p}. \quad (12)$$

Now, since for a fractal the number of sites in a box with linear dimension l behaves as $m(l) \sim l^{d_f}$ (i. e., d_f is the fractal dimension defined through box-counting), $M_{p+1}/M_p = (L^{p+1}/L^p)^{d_f} = L^{d_f}$, and the last equation can be rewritten as

$$\frac{D_p}{D_{p+1}} = L^{d_f-2} \frac{\Delta V_{p+1}}{\Delta V_p}, \quad (13)$$

As previously shown [7, 8], a perfect diffusive self-similar structure corresponds to a ratio D_p/D_{p+1} which does not depend on p , i. e.,

$$\frac{D_p}{D_{p+1}} = 1 + \lambda, \quad (14)$$

with λ a positive constant. In this model, the mean-square displacement for a single random walker behaves as

$$\Delta^2 x(t) = f(t)t^{2\nu}. \quad (15)$$

The modulation $f(t)$ is a log-periodic function, $f(t\tau) = f(t)$, and both ν and τ can be analytically calculated in terms of L and λ :

$$\nu = \frac{1}{2 + \frac{\log(1 + \lambda)}{\log(L)}} \quad (16)$$

$$\tau = L^{1/\nu} \quad (17)$$

The important partial conclusion in the context of this work is that, according to above discussion, a perfect diffusive self-similar structure implies a power-law behaviour for the resistance as a function of length. Indeed, equations (13) and (14) leads to

$$\frac{\Delta V_{p+1}}{\Delta V_p} = L^{1/\nu - d_f}, \quad (18)$$

where we have used $1 + \lambda = L^{1/\nu - 2}$, from equation (16). Thus, for a perfect diffusive self-similar fractal the potential difference, which corresponds to steady-state current, scales with length l as

$$\Delta V \sim l^\zeta, \quad (19)$$

where the exponent ζ is given by

$$\zeta = 1/\nu - d_f; \quad (20)$$

which is the Einstein relation (2), with $d_w = 1/\nu$.

4. Local exponents

We consider now a generic substrate for which diffusive self-similarity is reached only asymptotically. Let us assume a ratio between consecutive diffusion coefficients, that depends on the generation p , as

$$\frac{D_p}{D_{p+1}} = 1 + \lambda_p. \quad (21)$$

where, $\{\lambda_p : p = 1, 2, \dots\}$ is a sequence of non-negative real numbers, with $\lim_{p \rightarrow \infty} \lambda_p = \lambda$.

Because of this limit, at long enough times a single random walk on this substrate will show a MSD behaviour as in equation (15), and, as pointed out before, for large

enough lengths the potential difference will behave as in equation (19); with ν and ζ given by equations (16) and (20).

In this section we focus on local exponents, which correspond to the slopes in log-log scales for finite length or time. As shown for example in [8], on a substrate on which diffusion coefficients for generations p and $p + 1$ satisfy equation (21), the MSD for a single random walker behaves as

$$\Delta^2 x(t) \sim t^{2\nu_p}, \quad \text{for } L^p \lesssim \Delta x \lesssim L^{p+1}, \quad (22)$$

with the local exponent ν_p given by

$$\nu_p = \frac{1}{2 + \frac{\log(1 + \lambda_p)}{\log(L)}}. \quad (23)$$

Then, after rearranging this equation as $1 + \lambda_p = L^{1/\nu_p - 2}$, which corresponds to the left hand side of equation (13), we obtain

$$\frac{\Delta V_{p+1}}{\Delta V_p} = L^{1/\nu_p - d_f}. \quad (24)$$

Thus, we expect that the potential difference scales with length l as

$$\Delta V(l) \sim l^{\zeta_p}, \quad \text{for } L^p \lesssim l \lesssim L^{p+1}, \quad (25)$$

and that the local exponents satisfy the relation

$$\zeta_p = 1/\nu_p - d_f. \quad (26)$$

Therefore, local slopes in log-log scales for the resistance as a function of length and for MSD of a single random walker as a function of time are related for all scales through equation (26); which generalizes the Einstein relation.

5. Numerical simulations

We study numerically the steady-state that corresponds to a unitary current on two models, for which diffusive self-similarity appears asymptotically. At finite lengths, the local random-walk exponent ν_p is not constant. Thus, we expect an also variable resistance exponent ζ_p , related to the former through equation (26).

The first model is a substrate built on a square lattice. A random walk consists in a particle hopping among NN sites. If sites are connected by a bond, the hopping rate is $k = 1/4$. If the sites are not connected, the hopping rate is $k = 0$. A fractal is obtained by deleting some bonds. The characteristic scale factor is $L = 3$, and the unit cells for the first, the second and the third generations are depicted schematically in figure 3. For every generation the unit cell can be separated from the rest by cutting four bonds. As shown in a previous work, the mass on this structure shows a power-law behaviour with $d_f = 2$. However, the random walk exponent ν_p grows with time and approaches a value $\nu < 1/2$ when $t \rightarrow \infty$ [8].

We have run numerical simulations on the unit cell of the sixth generation, to reach the steady-state in which a unitary current flows between the left and right extremes. In figure 4 we plot with symbols the potential differences for lengths $x = 3^i$ ($i = 0, 1, \dots, 6$), which are the unit cell linear sizes for the generations zero to six. In the same figure, we plot a line using the relation (26) and the numerical values for ν_p , which are the outcomes of random walk simulations reported in reference [8]. Notice that both data set fall on the same curve, which confirms the relation (26).

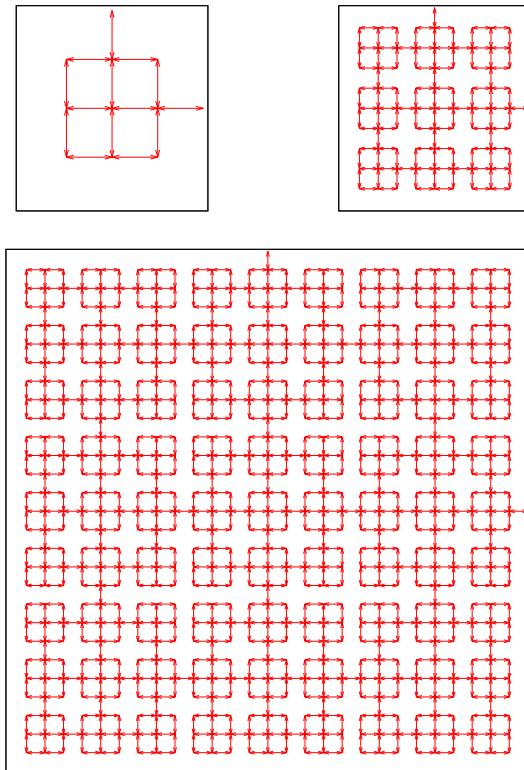


Figure 3. Substrate in two dimensions, which results in scale-dependent walk and resistance exponents. The schematics correspond to the unit cells for the first, second and third generations. The segments represent bonds between sites.

The second model is a generalization of the one-dimensional self-similar model introduced in [7]. We start with a single random walk on a one-dimensional lattice, with a hopping rate k_0 between any pair of NN sites. This homogeneous case corresponds to generation zero. We introduce a natural number L to build the other generations.

In the first generation, we reset to $k_1 < k_0$ the hopping rate for every pair of sites j and $j + 1$, with $\text{mod}(j, L) = 0$. The other hopping rates remains as in zeroth generation.

In the second generation, we reset to $k_2 < k_1$ the hopping rate for every pair of sites j and $j + 1$, with $\text{mod}(j, L^2) = 0$. The other hopping rates remains as in first generation.

This recursion follows indefinitely, in such a way that generation n is obtained from generation $n - 1$ after resetting to $k_n < k_{n-1}$ the hopping rate for every pair of sites j and $j + 1$, with $\text{mod}(j, L^n) = 0$. In figure 5 we show an schematics for $L = 5$.

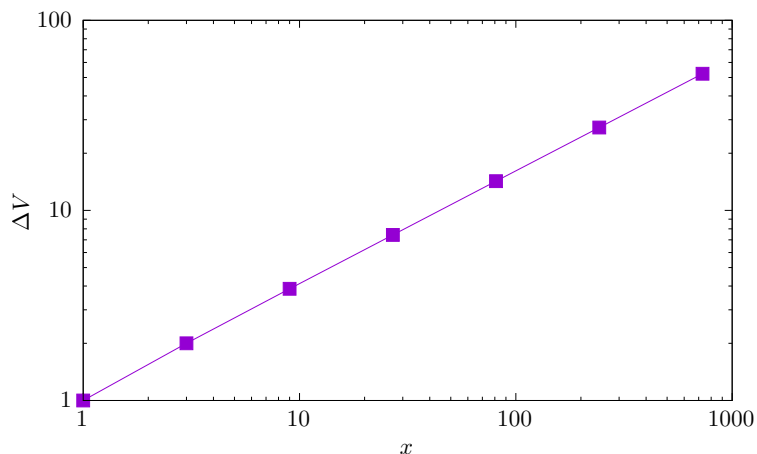


Figure 4. Potential difference as a function of length for a unitary current flowing through the unit cell of the sixth generation substrate in figure 3. The symbols correspond to simulations of the steady-state. The line was plotted with the exponents ζ_p from equation (26) and the values of ν_p which result from random-walk numerical simulations.

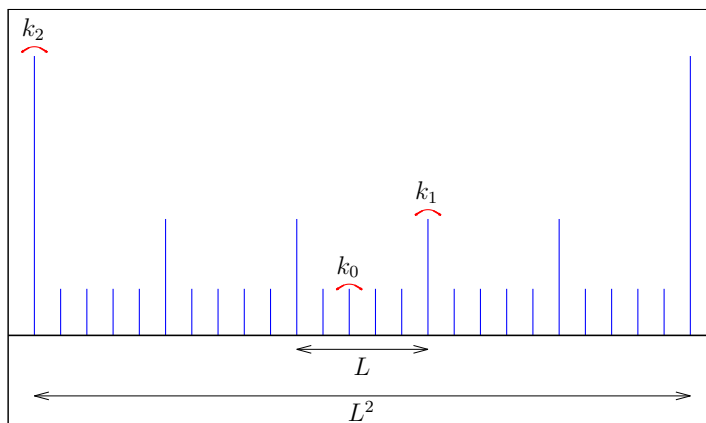


Figure 5. Schematics of the one-dimensional random-walk model. We begin with a homogeneous lattice, and a hopping rate k_0 between nearest-neighbor sites. Then, hopping rates are reset to k_j for transitions between sites j and $j + 1$ for every j such that $\text{mod}(j, L^n) = 0$, and for $n = 1, 2, \dots$. In this example, $L = 5$.

If we ask for perfect self-similarity for diffusion, i. e. equation (14), the hopping rates are found iteratively as in reference [7]. For the more general case of equation (21), the sequence of hopping rates is given by

$$\frac{1}{k_i} = \frac{1}{k_{i-1}} + \frac{L^i \lambda_{i-1}}{k_0} \prod_{j=0}^{i-2} (1 + \lambda_j), \quad \text{for } i = 1, 2, 3, \dots \quad (27)$$

We test the validity of the relation (26) among the local exponents for a family of

substrates given by

$$\lambda_p = \lambda(1 - 2^{-p/5}). \quad (28)$$

At short enough lengths these substrates are nearly homogeneous ($\lambda_p \approx 0$ for $p \ll 5$), while, on the other extreme, self-similarity for diffusion is reached for lengths much larger than L^5 . The local random walk exponent (23) decreases with length and approaches asymptotically ν in equation (16). Thus, the variation of ν_p in space increases with λ and, because of equation (26), the same should occur with the variation of ζ_p . This is an interesting model, because the variation of the exponents with length can be adjusted through the parameter λ .

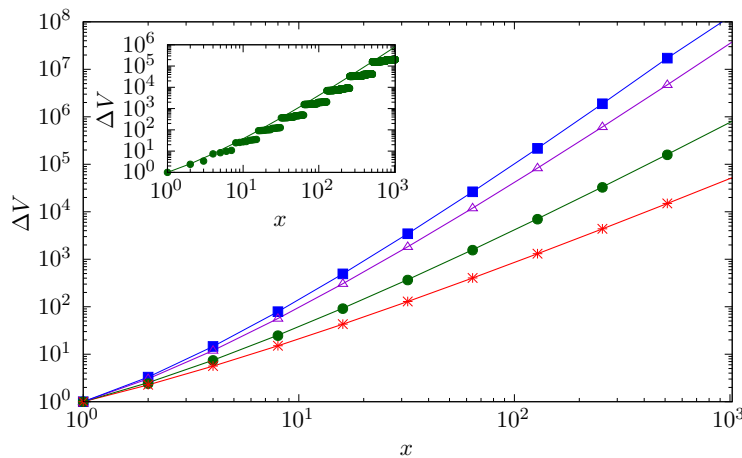


Figure 6. Potential difference as a function of length for unitary current on the one-dimensional model with $\lambda_p = \lambda(1 - 2^{-p/5})$, and $L = 2$. (Main) Symbols correspond to data obtained with numerical simulations on a tenth-generation substrate. Lines were drawn using the values of theoretical exponents. From bottom to top, $\lambda = 1$ (red), $\lambda = 2$ (green), $\lambda = 4$ (violet), $\lambda = 5$ (blue). (Inset) More detailed structure for $\lambda = 2$.

We have run numerical simulations for the steady-state that corresponds to a unitary current flowing on this model, with $L = 2$ and $\lambda = 1, 2, 4, 5$. All substrates were built until generation 10. In figure 6-main we plot with symbols the potential difference as a function of the length x , for $x = 2^j$ ($j = 0, 1, \dots, 9$). The lines correspond to the exponents ζ_p obtained from equations (26) and (23). Note the excellent agreement between theory and simulations. The inset in the same figure shows substructure of ΔV for $\lambda = 2$.

6. Conclusions

We have studied first the connection between single random walks and steady-state potential difference for substrates with spatial periodicity. Then, by considering a sequence of periodic systems, a common procedure for deterministic fractal construction, we find that the length dependent fractal, walk and resistance exponents, for the

substrate obtained in the infinite limit of this sequence, satisfy, at every length scale, the relation (26). This can be considered as a local version of the Einstein relation (2). We have tested our predictions numerically for two models. The first model is a fractal in two dimensions, while the second is a fractal in one dimension. Both models lead to length-dependent exponents at intermediate scales. The excellent agreement between the outcomes of these simulations and the theoretical predictions supports the validity of the mentioned relation among exponents, not only in the asymptotic self-similar limit but also locally, for all length scales.

Acknowledgments

We are grateful to H. O. Martín for useful discussions. This research was supported by the Universidad Nacional de Mar del Plata, 15/E1040, and the Consejo Nacional de Investigaciones Científicas y Técnicas, PIP1748/21.

References

- [1] Peter J. Grabner and Wolfgang Woess. Functional iterations and periodic oscillations for simple random walk on the sierpinski graph. *Stochastic Processes and their Applications*, 69(1):127 – 138, 1997.
- [2] L. Acedo and S. B. Yuste. Territory covered by n random walkers on fractal media: The sierpinski gasket and the percolation aggregate. *Phys. Rev. E*, 63:011105, Dec 2000.
- [3] M. A. Bab, G. Fabricius, and E. V. Albano. On the occurrence of oscillatory modulations in the power law behavior of dynamic and kinetic processes in fractals. *EPL (Europhysics Letters)*, 81(1):10003, 2008.
- [4] M. A. Bab, G. Fabricius, and Ezequiel V. Albano. Revisiting random walks in fractal media: On the occurrence of time discrete scale invariance. *The Journal of Chemical Physics*, 128(4):–, 2008.
- [5] Alberto L. Maltz, Gabriel Fabricius, Marisa A. Bab, and Ezequiel V. Albano. Random walks in fractal media: a theoretical evaluation of the periodicity of the oscillations in dynamic observables. *Journal of Physics A: Mathematical and Theoretical*, 41(49):495004, 2008.
- [6] Sebastian Weber, Joseph Klafter, and Alexander Blumen. Random walks on sierpinski gaskets of different dimensions. *Phys. Rev. E*, 82:051129, Nov 2010.
- [7] L. Padilla, H. O. Martín, and J. L. Iguain. Log-periodic modulation in one-dimensional random walks. *EPL (Europhysics Letters)*, 85(2):20008, January 2009.
- [8] L. Padilla, H. O. Martín, and J. L. Iguain. Log-periodic oscillations for diffusion on self-similar finitely ramified structures. *Phys. Rev. E*, 82:011124, Jul 2010.
- [9] L. Padilla, H. Martín, and J. Iguain. Anomalous diffusion with log-periodic modulation in a selected time interval. *Physical Review E*, 83(2):2–5, feb 2011.
- [10] Daniel ben Avraham and Shlomo Havlin. *Diffusion and Reactions in Fractals and Disordered Systems*. Cambridge University Press, 2000.
- [11] Bernhard Krön and Elmar Teufl. Asymptotics of the transition probabilities of the simple random walk on self-similar graphs. *Trans. Amer. Math. Soc.*, 356:393–414, 2004.
- [12] L. Padilla, H. O. Martín, and J. L. Iguain. Anisotropic anomalous diffusion modulated by log-periodic oscillations. *Physical Review E*, 86(1):011106, jul 2012.
- [13] Frechero, M. A., Padilla, L., Martín, H. O., and Iguain, J. L. Intermediate-range structure in ion-conducting tellurite glasses. *EPL*, 103(3):36002, 2013.
- [14] Amin Bunde and Shlomo Havlin (Eds.). *Fractals and Disordered Systems*. Springer, 1996.

- [15] J A Given and B B Mandelbrot. Diffusion on fractal lattices and the fractal einstein relation. *Journal of Physics A: Mathematical and General*, 16(15):L565, oct 1983.
- [16] Astrid Franz, Christian Schulzky, and Karl Heinz Hoffmann. The Einstein relation for finitely ramified Sierpinski carpets. *Nonlinearity*, 14(5):1411, aug 2001.
- [17] Alberto L Maltz, Gabriel Fabricius, Marisa A Bab, and Ezequiel V Albano. Random walks in fractal media: a theoretical evaluation of the periodicity of the oscillations in dynamic observables. *Journal of Physics A: Mathematical and Theoretical*, 41(49):495004, oct 2008.
- [18] András Telcs. The Einstein Relation for Random Walks on Graphs. *Journal of Statistical Physics*, 122(4):617–645, 2006.
- [19] Martin Hendrick and Philippe Renard. Fractal dimension, walk dimension and conductivity exponent of karst networks around tulum. *Frontiers in Physics*, 4, 2016.
- [20] C. M. Aldao, J. L. Iguain, and H. O. Martín. Diffusion of tagged particle in an exclusion process. *Surf. Sci.*, 366:483–490, Apr 1996.